New Investigation of Tidal Gravity Results from the GGP Network

Bernard Ducarme*, He-Ping Sun**and Jian-Qiao Xu**
**Chercheur Qualifié au FNRS, Observatoire Royal de Belgique*
Av. Circulaire 3, B-1180 Brussels, email: b.ducarme@ksb-orb.oma.be
***Institute of Geodesy and Geophysics, Chinese Academy of Sciences*
54 Xu Dong road, 430077 Wuhan, China, email: heping@asch.whigg.ac.cn

Abstract

Some 20 series longer than one year are now available in the GGP data bank, including 3 dual sphere instruments. To eliminate the tidal loading effects we interpolated the contribution of the smaller oceanic waves from the 8 well determined ones i.e. Q_1, O_1, P_1, K_1, N_2, M_2, S_2 and K_2. It was done for six different oceanic models: SCW80, CSR3.0, FES95.2, TPXO2, CSR4.0 and ORI96. In the diurnal band no model is decisively better than the others and a mean tidal loading vector is giving the most stable solution for the study of the liquid core resonance. In the semi-diurnal band however the SCW80 and TPXO2 models are not convenient.

We are investigating mainly the diurnal waves around the liquid core resonance i.e. K_1, y_1 and j_1. The scattering of the corrected amplitude factors for the waves O_1 and K_1 reaches 0.3%. and the tidal factors are determined with a precision slightly better than 0.1%. O1 is fitting perfectly to the DDW99 and MAT01 models but there is an offset of 0.1% for K_1. K1 exhibits a slight phase advance with respect to O1.

From our data set we computed the FCN period and found values very close to the 429.5 days deduced from the VLBI observations.

1. Introduction

Since July 1997 more than 15 superconducting gravimeters are operating in the framework of the Global Geodynamics Project (GGP) (Crossley & al.,1999), following to standardised procedures. Nineteen stations with data sets longer than one year are now available in the GGP data bank, hosted at the Royal Observatory of Belgium, including 3 dual sphere instruments. The one minute sampled original data obtained are pre-processed and analysed at the International Centre for Earth Tides (ICET) using the standard procedures (Ducarme & Vandercoilden, 2000). These data are corrected using a remove restore technique based on the T-soft software (Vauterin, 1998) and decimated to one hour sampling prior to the analysis by ETERNA software (Wenzel, 1996). Atmospheric pressure is the only auxiliary channel available for all the stations. For the dual sphere (CD) instruments the results of the U and L spheres are so close that we computed a common analysis of the two time series. For the stations Strasbourg and Wettzell we consider also the series obtained with the old T005 and T103 instruments. Finally we introduced the results of the renovated ASK228 gravimeter of Pecny (BroZ & al., 1996) which has an RMS error on the unit weight better than many of the oldest cryogenic instruments. Altogether we are thus considering 22 data sets, 10 or them outside Europe. For each of them we are able to extract 22 tidal groups: s_1, Q_1, r_1, O_1, NO_1, p_1, P_1, K_1, y_1, j_1, q_1, J_1, OO_1, $2N_2$, m_2, N_2, n_2, M_2, L_2, T_2, S_2, K_2.

In table 1 we give the details of the different series in increasing ICET station number, which allows to see the regional distribution of stations. For recent instruments, CT or CD series, the RMS error on the unit weight is below one $nm.s^{-2}$. In Potsdam we have the only T model with an error below $1nms^{-2}$.

The barometric efficiency is always close to $-3nms^{-2}$/hPa with three exceptions: the Askania gravimeter at Pecny, a very low coefficient at Sutherland and a very high one at Syowa. For the 19 other series we have as a mean: 3.368 ± 0.036 nms^{-2}/hPa, with a standard deviation s = 0.152 nms^{-2}/hPa.

Table 1 Characteristics of the tidal gravity stations

T: large dewar, CT: compact, CD : dual sphere, ASK: Askania

GGP	ICET	name	Lat.	Long.	Instr.	Data set (days)	RMS error	Baro. Fact. (nms^{-2}/hPa)
BE	0200	Brussels	50.7986	4.3581	T003	6,660	1.743	-3.467±.005
MB	0243	Membach	50.6093	6.0066	CT21	1,728	1.007	-3.286±.006
ST	0306	Strasbourg	48.6223	7.680	T005	3,272	2.265	-3.128±.010
					CT26	817	0.797	-3.394±.007
BR	0515	Brasimone	44.1235	11.1183	T015	1,098	2.576	-3.053±.036
VI	0698	Vienna	48.2493	16.3579	CT25	729	0.662	-3.467±.007
WE	0731	Wetzell	49.1458	12.8794	T103	726	2.639	-3.374±.031
					CD029	2x291	0.667	-3.340±.009
PO	0765	Potsdam	52.3809	13.0682	T018	2,250	0.855	-3.313±.004
MO	0770	Moxa	50.6450	11.6160	CD34	2x580	0.590	-3.320±.005
ME	0892	Metsahovi	60.2172	24.3958	T020	1614	1.299	-3.636±.007
PC	0930	Pecny	49.9200	14.780	*ASK228*	412	0.887	*-4.894±..013*
WU	2647	Wuhan	30.5139	114.4898	CT32	985	0.750	-3.237±..010
KY	2823	Kyoto	35.0278	135.7858	T009	686	3.323	-3.183±..038
MA	2824	Matsushiro	36.5430	138.2070	T011	880	1.163	*-3.523±..006*
ES	2849	Esashi	39.1511	141.3318	T007	875	1.286	-3.549±..011
SU	3806	Sutherland	-32..3814	20.8109	CD37	(491+304)	0.689	*-2.657±..013*
BA	4100	Bandung	-6.8964	107.6317	T008	420	7.450	-3.524±..243
CB	4204	Canberra	-35.3206	149.0077	CT31	890	0.776	-3.392±..010
BO	6085	Boulder	40.1308	254.7672	CT024	1,401	0.997	-3.518±..007
CA	6824	Cantley	45.5850	284.1929	T012	2,386	1.443	-3.293±..006
SY	9960	Syowa	-69.0070	39.5950	T016	548	1.103	*-4.115±.009*

Table 2 Stability of the tidal analysis results

Station	Instr.	Series	d(O_1)	d(K_1)	d(M_2)	d(S_2)	Discr.%
BE0200	T003	82/86	1.15375	1.14072	1.18404	1.19826	
		86/91	1.15290	1.13982	1.18334	1.19623	
		91/96	1.15338	1.13967	1.18410	1.19643	
		96/00	1.15344	1.14019	1.18379	1.19587	
							@0.1%
ME0243	CT21	95/97	1.14939	1.13730	1.18734	1.19285	
		98/00	1.14932	1.13734	1.18750	1.19225	
							<0.1%
ST0306	T005	87/91	1.14708	1.13520	1.18496	1.18750	
		91/96	1.14745	1.13535	1.18510	1.18794	<0.1%
	CT26	97/99	1.14871	1.13704	1.18657	1.18887	
							@0.1%
WE0731	T103	96/98	1.14424	1.13101	1.17973	1.17684	
	CD29	98/01	1.14820	1.13531	1.18357	1.18170	
							@0.4%
PO0765	T018	92/95	1.15003	1.13732	1.18607	1.18510	
		95/98	1.14966	1.13738	1.18592	1.18529	
							<0.1%
ME0892	T020	94/96	1.15317	1.14063	1.18178	1.17618	
		97/00	1.15304	1.14078	1.18090	1.17543	
							<0.1%
CA6824	T012	89/95	1.16655	1.14819	1.20434	1.18479	
		97/99	1.16530	1.14745	1.20270	1.18270	
							@0.1%

To study the stability of the tidal analysis results we subdivided the longest series on one hand and compared the results of different instruments in the same station on the other hand. From the results of Table 2 it is clear that, in each station, the tidal analysis factors of the main waves are stable at the 0.1% level with the exception of Wettzell. We shall see later on that it is the T103 which is not correctly calibrated. On the contrary at Strasbourg the renovated superconducting gravimeter agrees at the 0.15% level with the older series. As it could be expected the phase differences agree within 0°.5.
It should be pointed out that the internal analysis errors are lower by one order of magnitude.

2. Efficiency of the tidal loading correction

For tidal loading correction we are using 6 different tidal models: SCW80 (Schwiderski, 1980), CSR3.0 (Eanes, 1996), FES95.2 (Le Provost & al., 1994), TPXO2 (Egbert & al., 1994) , CSR4.0 and ORI96 (Matsumoto & al., 1995). Schwiderski is currently used as a working standard since more than 20 years but its coverage is not sufficient in many areas. CSR3 and FES95.2 have been recommended by Shum & al.(1996) and tested by Melchior & Francis (1996) on tidal gravity data.

As a first step we want to compare the efficiency of the different oceanic models for the reduction of the tidal loading influence in our data set.

For any tidal wave let us define:

- the residual vector **B**(B,b) expressing the difference between the observed tidal vector **A**(A_{obs},a) and the body tides vector **R**(A_{DDW},0) modelled using the Dehant, Defraigne and Wahr (DDW99) non-hydrostatic model (Dehant et al., 1999), with

$A_{obs} = A_{th}.d_{obs}$ and $A_{DDW} = A_{th}.d_{DDW}$, i.e. **B=A-R**.

- the final residual vector **X**(X,c) expressing the discrepancy between the **B** vector and the oceanic loading vector **L**(L,l), i.e. **X=B-L**.

We can also compute their relative importance as **B**/A_{th} and **X**/A_{th}.

On the other hand, for any tidal vector **A**, we can compute weighted mean vectors (**M**) for the Diurnal(D) and Semi-Diurnal(SD) families by the formula:

$\mathbf{M}_D = [2*\mathbf{A}(O1) + \mathbf{A}(P1) + 3*\mathbf{A}(K1)]/6$

$\mathbf{M}_{SD} = [2*\mathbf{A}(M2) + \mathbf{A}(S2)]/3$

The weight of the waves is proportional to their amplitude. It is justified by the fact that the signal to noise ratio in the tidal gravity recording as well as in the oceanic tidal models is directly proportional to the amplitude of the tidal constituent. In table 4 we express for each station the mean vectors $\mathbf{M}_{D,SD}$ (**B**/A_{th}) and $\mathbf{M}_{D,SD}$ (**X**/A_{th})

Table 3. Global comparison of the efficiency of the different oceanic models

	SCW80	CSR3.0	FES95.2	TPX02	CSR4.0	ORI96	**MEAN**	
	%	%	%	%	%	%	**%**	N
Diurnal	88.8	93.1	96.3	95.9	94.7	93.0	**95.8**	6
emi-Diurnal	*82.5*	93.6	94.6	*77.6*	88.5	94.9	**91.7**	6
							94.2	4

For each wave we can define the efficiency of the tidal loading correction as (**B-X**)/**B**.
In a similar way the ratios are thus expressing the mean efficiency of the oceanic loading correction for the correspondent tidal family. As a first step we tried to determine a mean efficiency by averaging the results of all the stations for each oceanic model (Table 3). For the diurnal waves efficiencies are larger than 90% except for SCW80. In the semi-diurnal band however two models have a much lower efficiency, SCW80 and TPX02, and it was thus decided to exclude them for the detection of anomalous stations. Detailed investigations showed that it was mainly in Western Europe that these models were less efficient for tidal loading correction.

Table 4 . Efficiency $E_D = (M_D(\mathbf{B})-M_D(\mathbf{X}))/M_D(\mathbf{B})$ and $E_{SD} = (M_{SD}(\mathbf{B})-M_{SD}(\mathbf{X}))/M_{SD}(\mathbf{B})$ of tidal loading corrections bands
averaged in Diurnal and Semidiurnal bands for different oceanic models

Station		Diurnal waves, 6 oceanic models					Semi-Diurnal waves, 4 oceanic models*				
No.	Name	$M_D(\mathbf{B})$		$M_D(\mathbf{X})$		E_D	$M_{SD}(\mathbf{B})$		$M_{SD}(\mathbf{X})$		E_{SD}
		B(%)	b(°)	X(%)	c(°)	**%**	B(%)	b(°)	X(%)	c(°)	**%**
BE0200	Brussels	0.36	93..94	*0.39*	-28.54	*-7.6*	5.10	60.44	*0.50*	-70.84	**90.3**
MB0243	Membach	0.42	103.19	0.03	-55.20	**91.9**	4.73	56.15	0.15	-103.95	**96.9**
ST0306	StrasbourgT	0.46	127.69	0.16	-169.13	**66.3**	4.13	55.51	0.23	-120.24	**94.4**
	StrasbourgC	0.31	111.64	0.11	-79.75	**65.2**	4.14	53.15	0.29	-84.88	**92.9**
BR0515	Brasimone	0.59	146.84	*0.36*	-157.10	*39.1*	2.25	47.26	*0.56*	-118.43	**75.1**
VI0698	Vienna	0.43	139.07	0.14	-168.50	**66.9**	2.37	40.45	0.33	-120.14	**86.1**
WE0731	WetzellT	0.67	158.51	*0.48*	-169.57	*28.5*	2.68	51.83	*0.59*	-156.66	**78.2**
	WetzellC	0.58	108.94	0.22	100.03	**62.8**	3.40	52.72	0.39	109.45	**88.5**
PO0765	Potsdam	0.37	95.33	0.08	22.72	**78.7**	3.25	43.80	0.07	-57.85	**97.7**
MO0770	Moxa	0.41	111.83	0.03	124.34	**91.9**	3.34	48.34	0.19	-156.35	**94.4**
ME0892	Metsahovi	0.43	33.50	*0.54*	7.79	*-26.0*	2.01	30.91	0.27	-31.26	**86.6**
PC0930	Pecny	0.29	98.74	011	-14.71	**65.2**	2.62	38.76	0.42	-105.12	**84.1**
WU2647	Wuhan	2.16	-23.39	0.38	6.52	**82.5**	1.38	-27.53	0.29	-11.77	**79.3**
KY2823	Kyoto	5.27	2.85	0.24	57.55	**95.5**	4.12	1.88	0.12	104.35	**97.0**
MA2834	Matsushiro	4.77	4.91	0.19	-144.22	**96.0**	3.25	12.55	0.28	-120.98	**91.3**
ES2849	Esashi	6.67	11.98	*0.52*	-12.96	**92.2**	4.63	33.69	*0.63*	-11.005	**86.3**
SU3806	Sutherland	0.75	-57.46	0.24	-74.44	**68.5**	10.02	86.57	0.15	-29.47	**98.5**
BA4100	Bandung	20.88	93.94	*0.57*	-174.12	**97.2**	2.42	-37.40	*0.61*	102.27	74.6
CB4204	Canberra	1.85	-61.53	0.40	-2.57	**78.5**	4.64	-71.43	0.33	-84.23	**93.0**
BO6085	Boulder	3.00	60.87	0.22	49.00	**92.6**	0.48	77.14	0.27	-112.09	*43.4*
CA6824	Cantley	1.59	40.92	*0.49*	-8.42	**69.2**	3.84	-24.01	*0.62*	-107.37	**83.7**
SY9960	Syowa	8.23	5.95	*1.22*	-18.09	**85.2**	27.08	0.97	*6.36*	5.37	**76.5**

* SCW80 and TPX02 excluded

For well calibrated instruments large values of $M_{D,SD}(\mathbf{X})$ will correspond to imperfect loading correction. However large values of $M_{D,SD}(\mathbf{X})$ can also points to the stations with calibration errors, if the corresponding phase is close to 0° or 180°.

To detect calibration errors we averaged for each station the $M_{D,SD}(\mathbf{X})$ vectors of all the oceanic models, 6 in the diurnal band but only 4 in the semi-diurnal one..

In Table 4 the residues are scaled in function of the theoretical amplitude of the waves and are thus expressed in percentage. In the diurnal band the $M_D(\mathbf{B})$ residues are below 0.5% in Europe but reach 5% in Japan and up to 20% in Bandung, due to its very low latitude. In the semi-diurnal band the effect are decreasing from 5% to 2.5% from West to East in Europe. They are generally large elsewhere, except in Boulder. In Syowa and Sutherland the effects to be explained reach more than 10%.

Some series are clearly anomalous in both tidal families as Syowa and Bandung. It was expected in Syowa as the station is located at the Antarctic coast and for all the cotidal maps it is covered by water. For Bandung it is well known that Indonesian archipelago has very complex oceanic tides and it is not surprising that the oceanic loading evaluation not precise enough. The calibration is probably not in question as the final residue has a phase of 90°. In Boulder the very low efficiency of the tidal loading correction in SD is simply due to the fact that the loading amplitude is very low in this station.

In Europe the calibrations of Brasimone, Brussels and WetzellT are certainly questionable with final residues reaching 0.5%. Outside of Europe Esashi and Cantley seem also offset.

For further studies of the liquid core resonance effects we can conclude that, as previously noticed by Melchior & Francis (1996), no model is decisively better than the others in the diurnal band (Table 3) and that a mean tidal loading vector will probably give the most stable solution. The stations of Syowa and Bandung are probably to be rejected. A calibration error close to 0.5% is strongly suspected in Brussels(BE), Brasimone(BR), Cantley(CA), Esashi(ES) and WetzellT (WE,T103) and perhaps in Metsahovi(ME). Similar conclusions have been expressed by Baker & Bos (2001) using the FES99 oceanic model

3. Interpolated tidal loading effects

The tidal load vectors are directly proportional to the amplitude of the wave in the exciting tidal potential and the change of phase exhibits a regular behaviour with respect to the frequency shift. Figure 1 shows typical examples of the frequency dependant phase shift of the load vectors for different parts of the world. Therefore it is rather easy to interpolate the load vectors for the smaller components starting from the eight major components (Q1, O1, P1, K1, N2, M2, S2, K2). The load vectors have to be first normalised dividing by their theoretical amplitude in the tidal potential. However in the Diurnal band the most interesting weak components y_1 and j_1 need in fact to be extrapolated as they are outside of the frequency band extending from Q1 to K1.

Another difficulty is that the core resonance does also affect the oceanic tides (Wahr and Sasao, 1981). To assume a smooth behaviour we have thus first to correct this resonance effect on the main diurnal waves, especially K1, interpolate or extrapolate the weaker components and apply again the resonance on the results. The effect of the resonance is clearly seen on Figure 1.

This procedure has been applied on the real and imaginary parts of the oceanic load vectors computed using the 6 selected oceanic models. We computed 14 additional components: s_1, r_1, NO_1, p_1, y_1, j_1, q_1, J_1, OO_1, $2N_2$, m_2, n_2, L_2 and T_2. The efficiency of the ocean load corrections observed for the main tidal waves is confirmed for the weaker constituents which have been interpolated or even extrapolated. In the diurnal band the mean amplitude factor is uniformly reduced of 0.6% to 0.7% for all the waves and we are thus confident in the fact that our tidal loading correction is also improving the results of the small resonant waves y_1 and j_1.

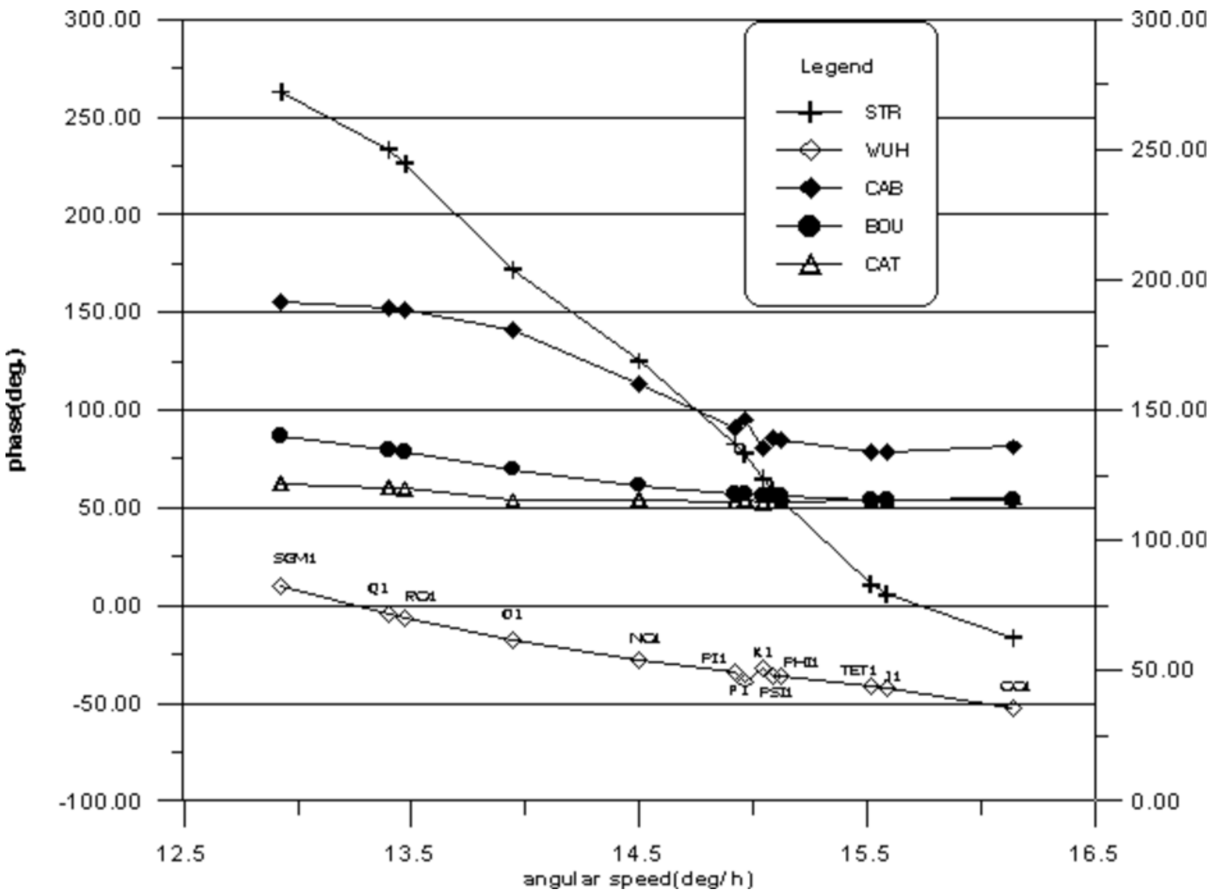

Figure 1. Phase shift of the oceanic load vectors(Diurnal band)
STR: Strasbourg, WUH: Wuhan, CAB: Canberra, BOU:Boulder, CAT: Cantley

4. Mean corrected tidal factors in the diurnal band

For each of the 13 diurnal wave groups we computed the corrected tidal gravity vectors $\mathbf{A_c}(d_c A_{th}, a_c)$ using the 6 tidal models, by the relation:

$$\mathbf{A_c}(d_c A_{th}, a_c) = \mathbf{A}(A_{obs},a) - \mathbf{L}(L,l)$$

Our main goal was to compute the best "mean" tidal factors for each wave group by averaging the six tidal models first and then the 22 series of observations. For each wave we constructed a double entry table similar to Table 5 and computed the mean value for each line or series. At this level it is important to reject the anomalous stations. In paragraph 2 we found several anomalous data sets. The problem is to know if they should be rejected beforehand. For station with suspicious calibration at the 0.5% level it is worth to point out that their effect is practically cancelling on the mean as we find three station with too low values(Brasimone, WetzellT and Bandung) and three with too high values (Brussels, Metsahovi and Esashi). Bandung is off set by more than 1% and has certainly to be rejected. On the other hand phase anomalies are also an important criterion to reject series. Moreover for the smaller constituents the noise level becomes a larger source of variability than an 0.5% calibration error, especially for stations with a large RMS error (Table 1). We decided thus to apply simply the criterion of the 3s level rejection on amplitude factors and phase differences for the 22 series. As expected Syowa was always rejected. Bandung was accepted for the largest constituents (K_1, O_1 and P_1). Kyoto was bad for all the small waves i.e. waves with amplitude lower than 2µgal at 45° or 5% of K1. Brasimone was rejected 6 times and a few other stations accidentally. For P_1 and K_1 we kept 21 data sets and as a minimum 17 for y_1. The lowest standard deviations are 0.3% on the amplitude factors and 0.08° on the phase differences for P_1 and K_1. It explains why only stations with a large calibration error will be rejected as for example Syowa in Table 7. For elimination due to the phase we see two examples in Table

5: Syowa and Wetzell C.

We can draw some interesting conclusions from Table 5. As already stated the mean observed tidal factor 1.1614 is reduced to 1.1544 and the discrepancy with the DDW99 model is thus reduced from 0.62% to 0.1%. We see also that the standard deviations on the lines are systematically different from the standard deviations on the columns . We computed the standard deviation of the mean corrected amplitude factor and phase difference (d_c = 1.1544, a_c = 0.01°) starting either from each series averaged over the 6 maps (column MEAN1) **s_1** or from the average of the 20 series for each map (line MEAN2) **s_2** and found very different results:

on d_c s_1 = 0.32% and s_2 = 0.07%

on a_c s_1 = 0.045° and s_2 = 0.025° .

If we consider that the variance on each element of the table is the same, the variance on the mean is divided by the number of elements i.e. 6 for a line or 20 for a column. The two standard deviations should then be in the ratio of the square roots i.e. 1.8. It is true for the phase differences with a ratio s_1 /s_2 = 1.8, but it is not true for the amplitude factor with a ratio 4.6 i.e. 2.5 times larger. On one hand it means that the dispersion due to the calibration errors in the stations is larger than the dispersion due the difference between the oceanic tidal models. On the other hand it confirms that the phase lag corrections are correct at the level of a few seconds.

In Table 6 we compare s_1 and s_2.(ÖN/6) and we see that this noise amplification for the d factors is true for all the waves except at the very edge of the spectrum for the waves S_1 and OO_1, where the extrapolation of the oceanic tides models increases the noise.

Table 5 Complete data set for wave O_1

Stations are ordered according to absolute value of latitude

Data sets	Observed		SCW80		CSR3.0		FES96.2		TPXO2		CSR4.0		ORI96	
	d	a	d	a	d	a	d	a	d	a	d	a	d	a
*SY9960	1.2690	.84	1.1814	-.11	1.1698	-.83	1.1625	.11	1.1685	.45	1.1596	-.87	1.1698	-.
ME0892	1.1531	.25	1.1567	.03	1.1570	.10	1.1566	.05	1.1577	.07	1.1591	.03	1.1653	.
PO0765	1.1499	.19	1.1537	.09	1.1543	.10	1.1536	.07	1.1547	.13	1.1544	.08	1.1547	.
BE0200	1.1533	.07	1.1566	.01	1.1577	.04	1.1569	-.02	1.1582	-.03	1.1574	-.04	1.1577	-.
MO0770	1.1487	.14	1.1527	.06	1.1534	.09	1.1525	.04	1.1534	.10	1.1534	.05	1.1535	-.
MB0243	1.1494	.11	1.1530	.05	1.1541	.08	1.1533	.02	1.1541	.06	1.1539	.02	1.1539	-.
PC0930	1.1489	.08	1.1526	.01	1.1535	.04	1.1524	-.01	1.1535	.03	1.1534	-.02	1.1537	-.
WE0731T	1.1442	.12	1.1480	.05	1.1489	.08	1.1479	.03	1.1488	.07	1.1488	.03	1.1490	-.
*WE0731C	1.1482	.23	1.1520	.17	1.1528	.19	1.1518	.14	1.1528	.19	1.1528	.15	1.1530	.
ST0306T	1.1472	.07	1.1515	.04	1.1524	.06	1.1513	.01	1.1522	.05	1.1521	.01	1.1523	-.
ST0306C	1.1487	.06	1.1530	.02	1.1539	.04	1.1528	-.01	1.1537	.03	1.1536	-.01	1.1538	-.
VI0698	1.1479	.10	1.1514	.03	1.1525	.05	1.1513	.00	1.1524	.05	1.1524	.00	1.1524	-.
CA6824	1.1663	.54	1.1590	-.01	1.1579	.05	1.1587	-.03	1.1590	-.05	1.1579	.01	1.1586	-.
BR0515	1.1462	.07	1.1500	.06	1.1508	-.01	1.1498	-.07	1.1496	.02	1.1504	-.05	1.1506	-.
BO6085	1.1642	1.31	1.1552	.15	1.1537	.08	1.1563	.02	1.1551	.02	1.1542	.04	1.1547	.
ES2849	1.2215	1.33	1.1540	-.09	1.1605	-.12	1.1623	.12	1.1619	.17	1.1580	-.06	1.1612	-.
MA2834	1.2043	.70	1.1486	-.13	1.1535	-.18	1.1535	.03	1.1542	.11	1.1529	.00	1.1541	-.
CB4204	1.1748	-.76	1.1593	-.14	1.1566	-.02	1.1541	-.16	1.157	.07	1.1567	.00	1.1575	.
KY2823	1.2097	.59	1.1523	-.01	1.1563	-.06	1.1558	.15	1.1543	.20	1.1547	.06	1.1567	-.
SU3806	1.1636	.12	1.1555	-.11	1.1535	-.16	1.1533	-.11	1.1554	.01	1.1533	-.10	1.1543	-.
WU2647	1.1793	-.38	1.1571	-.03	1.1590	-.15	1.1583	.08	1.1584	.14	1.1586	-.05	1.1588	-.
BA4100	1.1254	10.93	1.1587	*1.07	1.1586	.67	1.1460	.02	1.1528	-.66	1.1394	.16	1.1413	*1.
MEAN 2	1.1614	.010	1.1537	.004	1.1549	.039	1.1538	.012	1.1549	.030	1.1537	.008	1.1554	-.0
STD.DEV.			0.0032	.076	0.0029	.175	0.0038	.071	0.0032	.174	0.0043	.057	0.0038	.0

stations to be eliminated

	ampl.	phase
1	SY09960*	SY09960*
2		WE07313*

5. Comparison of the experimental results with different models

In table 6 we give the mean corrected tidal factors and phase differences for the 13 diurnal components and we compare them with several models DDW99 (non hydrostatic), MAT01 (Mathews, 2001) and several models obtained by fitting the data on a resonance model, using the waves O_1, P_1, K_1, y_1 and f_1 i.e.: SDX1, SDX2 and SDX3 (cfr §6 and Table 7). The models are normalised on O1 with d = 1.1544 and a = 0.0°.

In Table 6 we see that in fact these three models are very close when expressed in terms of amplitude factors and phase differences. On K1 the difference is only at the level of the fourth decimal, smaller than the associated RMS error on the tidal factor. Even on y_1 the difference is at the level of the experimental errors. As expected the SXD2 and SXD3 models, which are using directly the experimental values of Table 8, fit very well y_1, with a slight positive phase

For what concerns the comparison of the mean observed tidal factors with the DDW99 (non hydrostatic) and MAT01 models there are some contradictory remarks. These models are perfectly fitting O_1 at the level of the RMS errors, but are 0.1% too low with respect to K_1. In a previous reduction with 15 series(Ducarme & Sun, 2001) we already found a similar offset with $d(K_1) = 1.1356$. Concerning the slight phase advance of K_1 with respect to O1, forecasted by Mathews, no firm conclusion is possible as its magnitude is of the order of the associated RMS error on the phase differences. The positive result obtained in Ducarme & Sun (2001) is probably an artefact of the Schwiderski model in Western Europe. Concerning the small resonant waves y_1,and j_1 the RMS errors have been largely improved as, in the previous paper, we had only 9 selected stations, most of them in Europe. The model of Mathews fits better the observations and the experimental models, especially for j_1.

6. The Free Core Nutation

As already explained, we computed different solutions for the Free Core Nutation (FCN) deduced from our experimental data.

SDX1: stacking of the results of 19 stations (Sun & al., 2002)

SDX2: direct computation from the experimental results of table 8 with a weight inversely proportional to the RMS error on the amplitude factors s_1/ÖN

SDX3: direct computation from the experimental results of table 8 with a weight proportional to A_{th}.ÖN/s_1

The best solutions are obtained with the mean of the oceanic models (6 maps). The three solutions converge to the value deduced from the VLBI observations: 429.5 days.

It should be pointed out that the Mathews model is associated with a FCN period of 430,04 (429.93-430.48) days (Mathews & al.,2002). In the DDW99 model (Dehant & al., 1999) the FCN period was forced on 431 days, which was the value given by the VLBI observations at that time.

For SDX2 and SDX3 we also performed individual computations with the results obtained using each of the 6 oceanic models for loading corrections. These solutions are scattered between 425.3 and 435.6. CSR4.0 gives the minimum value and TPXO2 the maximum one. ORI96 provides also a too large value. The two approaches SXD2 and SXD3 are always very close.

Table 6 Mean tidal factors for the diurnal waves

	Mean factors		s_1	s_2*	DDW	MAT01	SXD1	SXD2	SXD3
Wave *N*	d_c *(e_d)*	a_c *(e_a)*	%	%		d *(a)*	d *(a)*	d *(a)*	d *(a)*
s_1	1.1550	0.164	0.47	0.52	1.1542	1.1541	1.15467	1.15467	1.15467
19	*±.0011*	*±.043*				*-0.028*	*0.000*	*0.000*	*0.000*
Q_1	1.1538	0.044	0.37	0.25	1.1543	1.1541	1.15458	1.15459	1.15459
20	*±.0008*	*±.026*				*-0.026*	*0.000*	*0.000*	*0.000*
r_1	1.1545	0.017	0.35	0.20	1.1543	1.1541	1.15457	1.15457	1.15457
17	*±.0009*	*±.048*				*-0.026*	*0.000*	*0.000*	*0.000*
·O_1	1.1544	0.010	0.32	0.13	1.1543	1.1540	1.15440	1.15440	1.15440
20	*±.0007*	*±.010*				*-0.024*	*0.000*	*0.000*	*0.000*
NO_1	1.1553	-0.023	0.58	0.20	1.1539	1.1535	1.15386	1.15385	1.15385
19	*±.0012*	*±.041*				*-0.021*	*0.000*	*0.000*	*0.000*
p_1	1.1510	-0.054	0.67	0.12	1.1507	1.1504	1.15091	1.15087	1.15087
17	*±.0016*	*±.091*				*-0.008*	*-0.002*	*-0.002*	*0.000*
P_1	1.1501	-0.039	0.29	0.13	1.1491	1.1489	1.14949	1.14953	1.14942
21	*±.0006*	*±.016*				*-0.002*	*-0.003*	*-0.003*	*0.000*
K_1	1.1362	0.025	0.31	0.11	1.1348	1.1349	1.13664	1.13643	1.13641
21	*±.0007*	*±.015*				*0.062*	*-0.004*	*-0.012*	*0.004*
y_1	1.2630	0.073	1.36	0.10	1.2717	1.2655	1.25993	1.26302	1.26217
16	*±.0034*	*±.230*				*0.022*	*0.360*	*0.071*	*0.110*
j_1	1.1691	0.061	0.79	0.25	1.1706	1.1693	1.16856	1.16878	1.16876
19	*±.0018*	*±.096*				*-0.068*	*0.016*	*0.010*	*0.002*
q_1	1.1569	0.097	0.79	0.24	1.1571	1.1564	1.15643	1.15646	1.15646
18	*±.0019*	*±.132*				*-0.028*	*0.002*	*0.001*	*0.000*
J_1	1.1557	0.014	0.52	0.27	1.1569	1.1562	1.15622	1.15625	1.15625
19	*±.0012*	*±.055*				*-0.027*	*0.001*	*0.001*	*0.000*
OO_1	1.1513	0.300	0.75	0.58	1.1563	1.1556	1.15557	1.15559	1.15559
18	*±.0017*	*±.071*				*-0.024*	*0.001*	*0.001*	*0.00*

N: number of series, s_1: standard deviation on series, s_2*= s_2.(ÖN/6) : normalised standard deviation on oceanic models, e : RMS errors on tidal factors, · reference for SXD models.

Table 7 Experimental models of the core resonance

Oceanic model	SXD1		SXD2		SXD3	
	T(days)	Q	T(days)	Q	T(days)	Q
6 maps	429.9	20769	429.1	-1725650	429.7	54871
SCW80	432.1	12760	428.3	280847	429.5	78378
CSR3.0	428.6	28503	429.1	-34855	429.3	-75594
FES95.2	432.9	17492	427.9	1467138	427.2	41093
TPXO2	425.9	16250	432.4	-31252	435.6	-117705
CSR4.0	434.7	-60940	425.9	1732741	425.3	43722
ORI96	434.6	9387	431.8	24732	433.3	15152

SXD: Sun-Xu-Ducarme (Sun & al., 2002b)

7. The semi-diurnal waves

We applied a similar procedure to compute mean tidal factors and phase differences for the 9 semi-diurnal components (Table 8).It seems that the extrapolation of the oceanic loading is less stable than in the diurnal band. Very large error bars are associated with $2N_2$ and μ_2, T_2 and $n2$ give satisfactory results but not L_2.
In table 8 we give the solutions using 6 and 4 tidal models respectively. The systematic difference of the results obtained using SCW80 and TPX02, already detected in §2, is fully confirmed. The standard deviation $s2$ is greatly reduced using only 4 models. For all the waves except K_2 there is a systematic increase of at least 0.1% after the suppression of the 2 models. For M2 the mean corrected tidal factors computed using SCW80 and TPX02 are 0.5% lower than the values obtained with the 4 other ones, which agree between themselves to within 0.05% The solution with 4 oceanic models agree with the reference value 1.1619 for the two major constituents M_2 and S_2.

For what concerns the phase differences they are close to zero for the frequency band ranging from N_2 to M_2, but there is a large systematic offset of -0.25° from L_2 to S_2.

It seems that the more turbulent characteristics of the semi-diurnal oceanic tides are responsible of the less stable solutions and increase the difference between the oceanic models. We should investigate more recent models such as FES99.

Table 8 Averaged tidal factors for the semi-diurnal waves

	Mean factors 6 maps		s1	s2*	DDW	Mean factors 4maps		s1	s2**
Wave *N*	d_c *(e_d)*	a_c *(e_a)*	%	%		d_c *(e_c)*	a_c *(e_c)*	%	%
$2N_2$	1.1623	-0.169	0.68	0.84	1.1619	1.1658	-0.247	0.83	0.20
13	*±.0019*	*±.132*				*±-.0023*	*±.166*		
m2	1.1609	-0.247	0.80	1.11	1.1619	1.1646	-0.306	1.06	0.26
19	*±.0018*	*±.0245*				*±.0024*	*±.155*		
N_2	1.1613	-0.086	0.35	0.81	1.1619	1.1631	-0.110	0.41	0.11
18	*±.0009*	*±.048*				*±.0009*	*±.033*		
n2	1.1598	-0.045	0.50	0.80	1.1619	1.1618	-0.036	0.40	0.16
21	*±.0011*	*±.035*				*±0.009*	*±.0034*		
M_2	1.1602	0.008	0.31	0.55	1.1619	1.1621	-0.009	0.28	0.11
19	*±.0007*	*±.021*				*±.0006*	*±.024*		
L_2	1.1604	-0.313	1.14	0.31	1.1619	1.1615	-0.297	1.18	0.16
16	*±.0029*	*±.099*				*±.0030*	*±.0092*		
T_2	1.1616	-0.360	0.51	0.35	1.1619	1.1625	-0.432	0.48	0.39
15	*±.0013*	*±.061*				*±.0012*	*±.066*		
S_2	1.1603	-0.229	0.16	0.34	1.1619	1.1614	-0.280	0.20	0.17
19	*±.0004*	*±.032*				*±0.004*	*±0.037*		
K_2	1.1634	-0.034	0.31	0.40	1.1619	1.1638	-0.114	0.35	0.38
20	*±.0007*	*±.047*				*±.0008*	*±.060*		

N: number of series, s_1: standard deviation on series, s_2*= s_2.(ÖN/6) : normalised standard deviation (6 oceanic models), s_2**= s_2.(ÖN/4) : normalised standard deviation (4 oceanic models), e : RMS errors on tidal factors.

8. Conclusions

We performed a careful study of the results obtained with superconducting gravimeters installed in 20 different stations, most of them belonging to the GGP network (Crossley et al., 1999). To take full advantage from the unprecedented precision of these data, it was necessary to compute tidal loading corrections not only for eight main waves (Q1, O1, P1, K1, N2, M2, S2, K2) but also for other weaker components, especially in the diurnal band near the liquid core resonance frequency. We had thus to interpolate or extrapolate the existing load vectors at neighbouring frequencies, taking into account the effect of the resonance itself on the oceanic tides, in order to keep only smooth functions of the frequency. We used 6 different tidal models SCW80, CSR3.0, FES96.2, TPXO2, CSR4.0 and ORI96.

To have an idea of the efficiency of these load corrections, we used weighted average of the main diurnal or semi-diurnal components to compute the discrepancy between the observed tidal vectors and the DDW99 non-hydrostatic model, before and after tidal loading correction. We found efficiencies close to 95% in the diurnal as well as the semi-diurnal band for the mean of the 6 tidal models. However SCW80 is less efficient in the two tidal bands and TPXO2 not convenient in the semi-diurnal one.

We found that there are still calibration errors at the 0.5% level in the GGP network. This fact is emphasised by the fact that, for most of the tidal waves, the standard deviation on the stations is 2.5 times larger than the standard deviation on the oceanic models.

We computed for 13 diurnal components mean values of the corrected amplitude factors and phase differences and compared them with several models of the FCN resonance.

The mean amplitude factor for O1 agrees perfectly with the DDW99 non-hydrostatic model as well as with the MAT01 model, but there is an offset of 0.1% on K1. The model of Mathews fits better the observed resonance. However we cannot confirm the predictions of the MAT01 model i.e. a slight phase advance for K1 and y_1,contrasting with a phase lag for j_1 as the RMS error on the phases is still too large. A phase very slight phase advance of K_1 is also found in the SXD3 model.

Different computations of the FCN period from our data set gave quite satisfactory results as we obtain periods comprised between 429.1 and 429.9 days, converging towards the value 429.5 days deduced from VLBI observations.

For the 9 semi-diurnal constituents the modelling is not good. SCW80 and TPX02 give too low corrected amplitudes factors (0.5% for M_2) and the interpolation procedure is not stable. It seems that the more turbulent characteristics of the semi-diurnal oceanic tides are responsible of less stable solutions and increase the differences between oceanic models.

Acknowledgements

The authors are grateful to D.Crossley , GGP Chairman, and all the GGP station managers: G.Casula (Brasimone, I), H.J.Dittfeld (Potsdam, D), M.&G.Harnisch (Wettzell, D), J.Hinderer (Strasbourg, F), Y.Imanishi(Matsushiro,JP), C.Kroner(Moxa,D), J.Merriam (Cantley, CDN), B.Meurers (Vienna,A), J.Neumeyer (Sutherland, SA), T.Sato(Esashi, JP and Canberra, AUS), K.Shibuya (Syowa, Antarctica), S.Takemoto (Bandung, Indonesia and Kyoto, JP), M.Van Camp (Membach, B), T.Van Dam and D.Crossley (Boulder, USA) and H.Virtanen (Metsahovi, SF). Z.Simon provided the excellent data set of Pecny, Czech Republic.

The authors wishes to express their thanks to M.Hendrickx and L.Vandercoilden, from the Royal Observatory of Belgium, who are maintaining the GGP data base at ICET and preprocessing all the incoming data before decimation to hourly intervals. This study was realised in the framework of the Bilateral Scientific and Technical Agreements between Belgium and China (project "SG observations and Geodynamics", BL/33/C17). H.P.Sun and J.Q. Xu are partly supported by the Natural Sciences Foundation of China, grants n^o 49925411 and 40174022.

References

Baker, T.F., Bos, M.S. (2001): Tidal gravity observations and ocean tide models. Proc. 14th Int. Symp. on Earth Tides, Journal of the Geodetic Society of Japan, **47**, 1, 76-81.

Broz, J., Simon Z., Zeman, A.(1997): Tidal station Pecny: Results of 20 years of observation with the gravimeters GS15 No 228. VUGTK, Proceedings of Research Work 1996, 75-88

Crossley, D., Hinderer, J., Casula G., Francis O., Hsu, H.T., Imanishi, Y., Jentzsch G., Kääriäinen J., Merriam, J., Meurers B., Neumeyer J., Richter B., Shibuya K., Sato T., Van Dam T. (1999): Network of superconducting gravimeters benefits a number of disciplines. EOS, **80**, 11, 121/125-126

Dehant, V., Defraigne, P. and Wahr, J. (1999): Tides for a convective Earth J. Geophys. Res., **104**, B1, 1035-1058.

Ducarme, B., Sun, H.P. (2001): Tidal gravity results from GGP network in connection with tidal loading and Earth response. Proc. 14th Int. Symp. on Earth Tides, Journal of the Geodetic Society of Japan, **47**, 1, 308-315.

Ducarme, B., Vandercoilden, L. (2000): First results of the GGP data bank at ICET. Proc. Workshop "High Precision Gravity Measurements with application to Geodynamics, March 24-26,1999. Cahiers du Centre Européen de Géodynamique et de Séismologie, **17**, 117-124.

Eanes, R., Bettadpur (1996): The CSR3.0 global ocean tide model: Diurnal and Semi-diurnal ocean tides from TOPEX/POSEIDON altimetry, CRS-TM-96-05, Univ. of Texas, Centre for Space Research, Austin, Texas

Egbert, G., Bennett, A., Foreman, M. (1994): TOPEX/Poseidon tides estimated using a global inverse model. Journal of Geophysical Research, **99**(C12), 24821-24852.

Le Provost, C., Genco, M.L., Lyard, F., Vincent, P., Canceil, P.(1994): Spectroscopy of the ocean tides from a finite element hydrodynamic model. Journal of Geophysical Research, **99**(C12), 24777-24797.

Mathews, P.M. (2001): Love numbers and gravimetric factor for diurnal tides. Proc. 14th Int. Symp. on Earth Tides, Journal of the Geodetic Society of Japan, **47**, 1, 231-236.

.Mathews, P.M., Herring, T.A., Buffett, B.A. (2002): Modeling of nutation-precession: New nutation series for nonrigid Earth and insights into the Earth's interior. Journal of Geophysical Research (under press).

Matsumoto, K., Ooe, M., Sato, T., Segawa, J. (1995): Ocean tides model obtained from TOPEX/POSEIDON altimeter data. J. Geophys Res., **100**, 25319-25330.

Melchior, P., Francis, O. (1996): Comparison of recent ocean tide models using ground-based tidal gravity measurements. Marine Geodesy, **19**, 291-330

Schwiderski, E.W. (1980): Ocean Tides I, Global ocean tidal equations. Marine Geodesy, **3**, 161-217.

Shum, C.K., Andersen, O.B., Egbert, G., Francis, O., King, C., Klosko, S., Le Provost, C., Li X., Molines, J.M., Parke, M., Ray, R., Schlax, M., Stammer D., Temey, C., Vincent P., Woodworth P.L., Wunsch C.(1996): Comparison of newly available deep ocean tide models by the TOPEX/POSEIDON Science Working Team. Journal of Geophysical Research

Sun, H.P., Ducarme, B., Xu, J.Q.(2002): Determination of the Free Core Nutation Parameters by Stacking Tidal Gravity Measurements from GGP network. Proc. GGP Workshop, Jena, March 11-15,2002.

Vauterin, P. (1998): Tsoft: graphical & interactive software for the analysis of Earth Tide data, Proc. Thirteenth Int. Symp. Earth Tides, Brussels, July 22-25 1997, Observatoire Royal de Belgique, Série Géophysique, 481- 486.

Wahr, J.M., Sasao, T. (1981): A diurnal resonance in the ocean tide and in the Earth's load response due to the resonant free core nutation. Geoph. J. R. Astr. Soc., **64**, 747-765.

Wenzel, H.G.(1996): The nanogal software: data processing package ETERNA 3.3, Bull. Inf. Marées Terrestres, **124**, 9425-9439.